IJMMM International Journal of Minerals, Metallurgy and Materials 矿物冶金与材料学报（英文版）

Recovery and separation of rare earth elements by molten salt electrolysis

Tai-qi Yin, Yun Xue, Yong-de Yan, Zhen-chao Ma, Fu-qiu Ma, Mi-lin Zhang, Gui-ling Wang, and Min Qiu

Cite this article as:
Tai-qi Yin, Yun Xue, Yong-de Yan, Zhen-chao Ma, Fu-qiu Ma, Mi-lin Zhang, Gui-ling Wang, and Min Qiu, Recovery and separation of rare earth elements by molten salt electrolysis, *Int. J. Miner. Metall. Mater.*, 28(2021), No. 6, pp. 899-914. https://doi.org/10.1007/s12613-020-2228-4

Articles you may be interested in

Chen-teng Sun, Qian Xu, Yan-ping Xiao, and Yong-xiang Yang, Electrochemical deposition of Nd and Nd–Fe alloy from Cu_6Nd alloy in a NaCl–KCl–$NdCl_3$ melt, *Int. J. Miner. Metall. Mater.*, 27(2020), No. 12, pp. 1650-1656. https://doi.org/10.1007/s12613-020-2130-0

Shi-yuan Liu, Yu-lan Zhen, Xiao-bo He, Li-jun Wang, and Kuo-chih Chou, Recovery and separation of Fe and Mn from simulated chlorinated vanadium slag by molten salt electrolysis, *Int. J. Miner. Metall. Mater.*, 27(2020), No. 12, pp. 1678-1686. https://doi.org/10.1007/s12613-020-2140-y

Xiao-li Xi, Ming Feng, Li-wen Zhang, and Zuo-ren Nie, Applications of molten salt and progress of molten salt electrolysis in secondary metal resource recovery, *Int. J. Miner. Metall. Mater.*, 27(2020), No. 12, pp. 1599-1617. https://doi.org/10.1007/s12613-020-2175-0

Shu-qiang Jiao, Han-dong Jiao, Wei-li Song, Ming-yong Wang, and Ji-guo Tu, A review on liquid metals as cathodes for molten salt/oxide electrolysis, *Int. J. Miner. Metall. Mater.*, 27(2020), No. 12, pp. 1588-1598. https://doi.org/10.1007/s12613-020-1971-x

Dong-yang Zhang, Xue Ma, Hong-wei Xie, Xiang Chen, Jia-kang Qu, Qiu-shi Song, and Hua-yi Yin, Electrochemical derusting in molten Na_2CO_3–K_2CO_3, *Int. J. Miner. Metall. Mater.*, 28(2021), No. 4, pp. 637-643. https://doi.org/10.1007/s12613-020-2068-2

Shao-chun Chen, Hong-xiang Ye, and Xin-qiang Lin, Effect of rare earth and alloying elements on the thermal conductivity of austenitic medium manganese steel, *Int. J. Miner. Metall. Mater.*, 24(2017), No. 6, pp. 670-674. https://doi.org/10.1007/s12613-017-1449-7

IJMMM WeChat

QQ author group

International Journal of Minerals, Metallurgy and Materials
Volume 28, Number 6, June 2021, Page 899
https://doi.org/10.1007/s12613-020-2228-4

Invited review

Recovery and separation of rare earth elements by molten salt electrolysis

Tai-qi Yin[1)], *Yun Xue*[1)], *Yong-de Yan*[1,2)], *Zhen-chao Ma*[3)], *Fu-qiu Ma*[1)], *Mi-lin Zhang*[1)], *Gui-ling Wang*[1)], *and Min Qiu*[2)]

1) Yantai Research Institute & Graduate School, Harbin Engineering University, Yantai 264006, China
2) College of Science, Heihe University, Heihe 164300, China
3) Zhongkexin Engineering Consulting (Beijing) Co., Ltd, Beijing 100039, China
(Received: 6 June 2020; revised: 18 November 2020; accepted: 19 November 2020)

Abstract: With the increasing demand of rare earth metals in functional materials, recovery of rare earth elements (REEs) from secondary resources has become important for the green economy transition. Molten salt electrolysis has the advantages of low water consumption and low hazardous waste during REE recovery. This review systematically summarizes the separation and electroextraction of REEs on various reactive electrodes in different molten salts. It also highlights the relationship between the formed alloy phases and electrodeposition parameters, including applied potential, current, and ion concentration. Moreover, the feasibility of using LiF–NaF–KF electrolyte to recover REEs is evaluated through thermodynamic analysis. Problems related to REE separation/recovery the choice of electrolyte are discussed in detail to realize the low-energy and high current efficiency of practical applications.

Keywords: rare earth element; molten salt; reactive electrode; electrochemical separation

1. Introduction

Rare earth elements (REEs) are of great economic importance because of their extensive applications in various functional materials, such as permanent magnets, catalysts, rechargeable batteries, and lamp phosphors. Given their excellent magnetic and electronic properties, REEs have become indispensable metals in our modern life. The increased demand and fragility of the supply chain have also made REEs critical metals in many countries [1]. The reserves of REEs in permanent magnets account for about 25% of the total production of rare earth elements. Nd–Fe–B magnets are widely used in many advanced applications, such as miniature high-capacity hard disk drives, magnetic resonance imaging, motors in hybrid electric vehicles (HEVs) and electric vehicles (EVs), efficient air conditioners, and wind turbines [2]. With the development of HEV and EV models in automotive manufacturers, the production of HEVs and EVs is forecast to exceed 10.1 million units in 2026 [3]. The life cycles of permanent magnets vary from 2–3 years in electronics to 20–30 years in wind turbines. Therefore, the recovery of REEs from end-of-life products is important to protect the environment and promote the sustainable development of rare earth resources.

REEs are traditionally recovered via hydrometallurgy [4], but this method has some drawbacks, such as using large amounts of chemicals and water and complicated, tedious, and time-consuming steps [5]. Therefore, pyrometallurgical (high-temperature) routes, including chemical vapor transport [6], selective reduction and distillation [7], selective chlorination and distillation [8], and liquid metal extraction [9], have served as alternatives to hydrometallurgical routes for recycling raw materials. Pyrometallurgical routes are characterized by the simultaneous separation and extraction of REEs. Among them, molten salt electrolysis has been extensively developed [10−12]. As a reaction medium, molten salts exhibit more advantages than water because of their high chemical stability, high conductivity, high reaction rates, broad range of applicable temperature, and low vapor pressure in different research fields, such as electrochemical reduction [13−14], electrochemical conversion of CO_2 [15−18], and oxide electrolysis [19−22].

Another important problem concerning molten salts is pyroprocessing for recycling of spent fuel. REEs are major fission products with a high thermal neutron capture cross section; hence, they complicate the control of reactor operation in the safe operation limits [23]. Accordingly, the separation of actinides and REEs in molten salts has been extens-

Corresponding authors: Yun Xue E-mail: xueyun@hrbeu.edu.cn; Yong-de Yan E-mail: y5d2006@hrbeu.edu.cn

ively studied by different countries [24−27].

The present review summarizes the essential fundamental parameters affecting the separation and extraction of REEs by using solid and liquid reactive electrodes. The separation factors for different electrodes and different molten salt systems are discussed and compared. The recovery efficiencies of REEs by different liquid electrodes in molten salt are also reviewed. The relationship between the types of intermetallic compounds and the preparation parameters are described. The feasibility of using LiF−NF−KF(FLiNaK) electrolyte for RE metal recovery is evaluated thermodynamically.

2. Separation and recovery of REEs on reactive electrodes

2.1. Description of separation/recovery on reactive electrodes

Moten salt electrolysis using an alloy diaphragm was proposed as a new developed process for the separation of rare earth metals [11]. The principle of molten salt electrolysis for the separation/recovery of rare earth metals is illustrated in Fig. 1 [28]. The recovery of REEs could be processed using molten salt electrolysis through four steps. First, an anode containing rare earth metals is dissolved into the molten salt. Second, the target metal ions are selectively deposited on the diaphragm surface to form rare earth alloys. Third, the target rare earth metal diffuses onto the surface of the cathode space through the alloy diaphragm and then dissolves into the molten salt as RE ion. Last, the target element is recovered as a rare earth metal or alloy on the cathode. During the experiment, the diaphragm serves as a "bifunctional" electrode and selectively permeates the target REE via molten salt electrolysis. In the anode space, the diaphragm (cathode) reacts with the deposited target metal ion to form an alloy in accordance with Eq. (1):

$$xA(III) + yB + 3xe^- \rightarrow A_xB_y \quad (1)$$

where A and B represent the REE and the substrate of reaction with the rare earth metal, respectively.

The rare earth metal can be chemically diffused through the diaphragm onto the surface of the cathode space and then dissolved into the molten salt as RE ions in accordance with Eq. (2):

$$A_xB_y \rightarrow zA(III) + A_{x-z}B_y + 3ze^- \quad (2)$$

However, the alloy diaphragm might crack or split because of the long processing time of electrolysis. Therefore, the concept of liquid electrode as a diaphragm was studied. As an example, the separation of Dy and Nd was performed in two steps, as shown in Fig. 2 [29]. In the first step, Dy and Nd in magnet scraps are dissolved into the molten salt as Dy(III) and Nd(III) ions, respectively. Meanwhile, Dy(III) is selectively deposited into the liquid electrode based on the applied potential or alloying rate. Subsequently, Dy atom is chemically diffused or transported onto the surface of the cathode space by mechanical stirring. In the second step, Dy metal in the Dy-based liquid alloy is dissolved as Dy(III) ion into the molten salt. The dissolved Dy(III) ion is deposited on an inert or reactive electrode to form a Dy metal or transition alloy. Therefore, the liquid metal serves as a bipolar electrode in the process.

In general, a three-electrode setup composed of working, counter, and reference electrodes is used to study the electrochemistry in molten salt, as shown in Fig. 3. Graphite rod serves as the counter electrode. For the reference electrode,

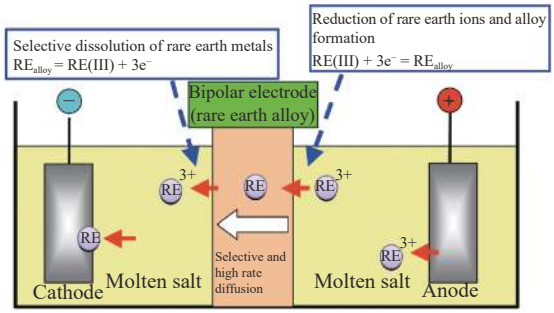

Fig. 1. Schematic of the separation and recovery of rare earth metals. Reprinted from H. Konishi, H. Ono, E. Takeuchi, T. Nohira, and T. Oishi, *ECS Trans.*, 61, 19-26(2014) [28]. © IOP Publishing. Reproduced with permission. All rights reserved.

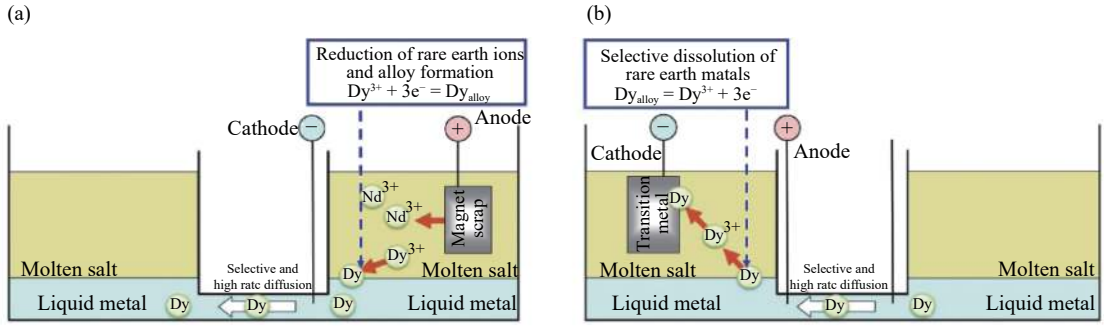

Fig. 2. Schematic of the (a) separation and (b) recovery of rare earth metals in the molten salt. Reprinted from A. Kuriyama, K. Hosokawa, H. Konishi, H. Ono, E. Takeuchi, T. Nohira, and T. Oishi, *ECS Trans.*, 75, 341-348(2016) [29]. © IOP Publishing. Reproduced with permission. All rights reserved.

Ag/AgCl is usually employed in molten chlorides, and Pt wire is used in molten fluorides [30]. The basic electrochemical properties could be measured on inert tungsten electrode. For the separation/extraction of REEs, some active metals in solid and liquid states at experimental temperature are selected as the reactive electrode [19,31].

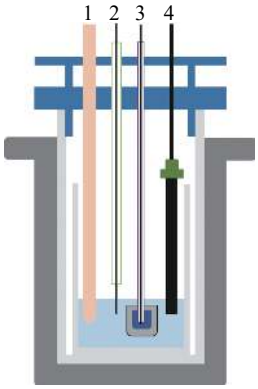

Fig. 3. Electrochemical cell for the recovery of rare earth metals on reactive electrode. 1—Reference electrode; 2—Solid working electrode; 3—Liquid working electrode; 4—Counter electrode.

2.2. Electrochemical alloying and dealloying on solid electrodes

2.2.1. Ni electrode

Electrochemical formation of Ni–Y intermetallic compound layer was investigated in LiCl–KCl–NaCl–YCl_3 melts [32], in which Ni_2Y, Ni_2Y_3, and NiY were prepared by galvanostatic electrolysis. Ni_2Y is the predominant Ni–Y intermetallic compound. Hachiya and Ito [33] performed a molecular dynamic simulation of the diffusion on the Ni_2Y intermetallic phase by using a nearly free electron tight-binding bond interatomic interaction model. In this case, the high growth rate of the Ni_2Y phase is owing to the high diffusion rate in and near the grain boundaries. Moreover, Han *et al.* [34] investigated the relationship between the alloy phase and the applied potential by electrolysis in LiCl–KCl–YCl_3 melts. The results indicate that Ni_2Y is the predominant Ni–Y intermetallic compound.

Considering the unknown mechanism for the formation of intermetallic compounds, Nohira *et al.* [35] systematically investigated the electrochemical formation and phase control of the Ni–Pr system. The Ni_2Pr phase was identified by potentiostatic electrolysis in LiCl–KCl–$PrCl_3$ melts at 0.5 V vs. Li/Li^+ for 0.5 h at 723 K. However, when the working electrode was changed to Ni_2Pr, various alloy phases were identified by varying the applied potentials. This processes involved are electrochemical implantation and dealloying [10]. Due to the rapid growth of the Ni_2Pr phase, the mechanism underlying the rapid formation of the Ni_2Pr phase was also discussed. A previous study [35] reported a linear relationship between Ni_2Pr thickness and electrolysis time and determined that the growth rate of Ni_2Pr is approximately 0.75 $\mu m \cdot min^{-1}$ within 10–120 min. The morphologies of Ni_2Pr characterized by transmission electron microscopy and electron diffraction confirmed that the growth rate of Ni_2Pr is overwhelmingly higher than that of other Ni–Pr phases, which is ascribed to the high Pr diffusivity in and near the grain boundaries.

Yin *et al.* [36] prepared Ni–Pr alloy in LiCl–KCl–$PrCl_3$ melts. Fig. 4 shows the SEM images of Ni–Pr alloys obtained by potentiostatic electrolysis at −1.75 and −1.9 V vs. Ag/Ag^+ for 2, 4, and 6 h at 943 K. The light gray and dark gray zones correspond to the Ni_2Pr intermetallic compound and the Ni matrix, respectively. The relationship between Ni_2Pr thickness and electrolysis time at different applied potentials is displayed in Fig. 5. The data show that the growth rate is faster than the linear rate and higher at a more negative potential.

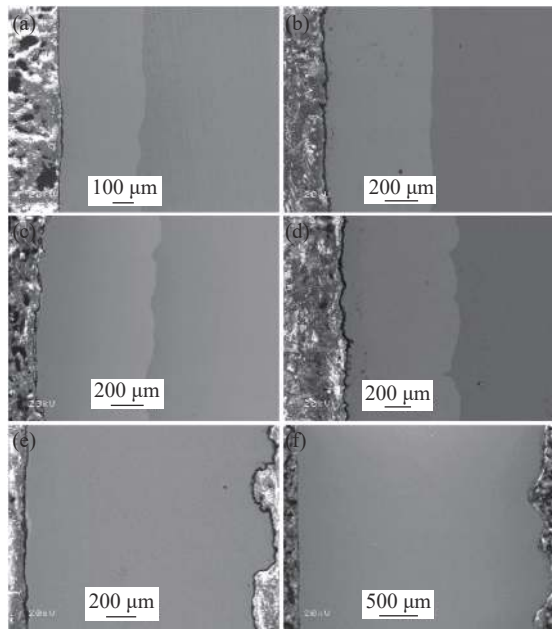

Fig. 4. SEM images of the samples prepared by potentiostatic electrolysis in LiCl–KCl–$PrCl_3$ melts: (a) 2 h, (c) 4 h, and (e) 6 h at −1.75 V; (b) 2 h, (d) 4 h, and (f) 6 h at −1.9 V. Reprinted from T.Q. Yin, Y. Liang, J.M. Qu, P. Li, R.F. An, Y. Xue, M.L. Zhang, W. Han, G.L. Wang, and Y.D. Yan, *J. Electrochem. Soc.*, 164, D835-D842(2017) [36]. © IOP Publishing. Reproduced with permission. All rights reserved.

Aside from Y and Pr, other REEs were studied on the Ni electrode in LiCl–KCl melts. These REEs include Sm–Ni [37−38], Tb–Ni [39], Dy–Ni [40], and Yb–Ni [41], where only Ni_2RE intermetallic compound is rapidly formed. Other Ni–RE alloy phases can also be prepared using Ni_2RE as the working electrode at various applied potentials. Moreover, different Ni_2RE alloys have a certain growth rate. On the basis of the results above, the separation of REEs was stud-

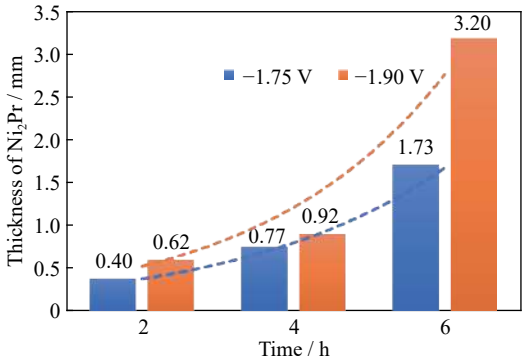

Fig. 5. Relationship between Ni_2Pr thickness and electrolysis time at different applied potentials.

ied using Ni electrode in LiCl–KCl melts. Konishi *et al.* [42] studied the separation of Tb from Nd in LiCl–KCl–$TbCl_3$–$NdCl_3$ melts at 723 K. In this case, the highest mass ratio of Tb/Nd in the alloy phase was calculated to be 56 at 0.7 V vs. Li/Li^+. The separation of Dy and Nd was carried out in LiCl–KCl melts by using a Ni-based alloy diaphragm [43]. The growth rate of Ni_2Nd is approximately 10 $\mu m \cdot h^{-1}$, which is lower than that of Ni_2Dy (28 $\mu m \cdot h^{-1}$). Thus, the difference in growth rate between Ni_2Nd and Ni_2Dy suggests the possibility of separating Dy in the LiCl–KCl–$DyCl_3$–$NdCl_3$ system. The highest mass ratio of Dy/Nd in the alloy phase was determined to be 72 at 0.65 V vs. Li/Li^+. For the separation of Dy from Nd and Pr, the highest mass ratio of Dy/(Nd + Pr) was found to be 50 at 0.65 V vs. Li/Li^+ in the LiCl–KCl–$DyCl_3$–$NdCl_3$–$PrCl_3$ system at 723 K [44]. On the basis of the results of REE separation on the Ni electrode, real Nd–Fe–B magnet scraps were employed in LiCl–KCl melts for recovery, and the mass ratio of Dy/Nd in the alloy phase was estimated to be 30 at 0.67 V vs. Li/Li^+ [45]. During the separation of Dy/Nd, the anodic current density reached the maximum value (280 A/m^2), and the permeation rate of Dy through an alloy diaphragm was evaluated to be 550 g/(m·h).

Yasuda *et al.* [46–49] systematically investigated the selective recovery of RE–Ni (RE = Pr, Nd, Dy) alloy in NaCl–KCl melts. Different alloy phases were formed by varying the applied potentials with Ni_2RE electrode in NaCl–KCl melts. The separation factors are defined as $\left[x_{Dy}/(x_{Pr}+x_{Nd})\right]_{alloy}$ (where x_{Dy}, x_{Pr}, and x_{Nd} are the mole fractions of Dy, Pr, and Nd) and found to be 9.9 and 22.9 at 0.42 and 0.45 V vs. Na/Na^+, respectively.

Compared with chloride melts, LiF–CaF_2 eutectic melts were selected as the electrolyte because of their high negative potential window [12]. The electrochemical formation behaviors of Pr–Ni [48], Nd–Ni [12], and Dy–Ni [50] were studied in LiF–CaF_2 melts. The result is the same as that in chloride melt, where the Ni_2RE phase is rapidly formed. In addition, Nd, Gd, and Dy were extracted on the reactive Ni and Cu electrodes in molten fluorides, and the extraction efficiencies of Nd and Gd were more than 99.8% [51–54]. Temperature plays a key role in enhancing the diffusion rate of rare earth metals on reactive electrodes. On the basis of the fundamental data of RE–Ni (RE denotes Pr, Nd, and Dy) alloy in LiF–CaF_2 melts, the effective electrolysis potential was suggested to be 0.34–0.4 V vs. Li/Li^+ for the separation of Dy from Nd and Pr [50]. However, the maximum Dy/Nd mass ratio in the alloy phase is only 5.6 in fluoride melts, which is much lower than that (121) in chloride melts [55].

2.2.2. Mg electrode

Yang *et al.* [56] selectively electrodeposited Dy from LiCl–KCl–$GdCl_3$–$DyCl_3$ melts on Mg electrode at 773 K; in this case, only Mg_3Dy was observed. The inductively coupled plasma atomic emission spectrometer (ICP–AES) rarely detected Gd in the deposited samples, and the extraction efficiency of Dy reached 98.4%. In addition, the growth rate of Mg_3Dy exceeded 20 μm/h in the first 12 h and then gradually decreased. The separation of Pr from Er could also be achieved in the LiCl–KCl–$PrCl_3$–$ErCl_3$ system [57], where the extraction efficiency of Pr reaches 95.3% at −1.9 V vs. Ag/Ag^+ under 823 K. The Mg electrode might be a promising candidate as a diaphragm for the separation and recovery of REEs.

The electrochemical preparation of Mg–RE alloy film was also studied in the LiCl–KCl–$RECl_3$ system. Potentiostatic electrolysis of LiCl–KCl–$LaCl_3$ melts at 873 K can produce various Mg–La intermetallic compounds, including $Mg_{17}La_2$ at −1.8 V, $Mg_{17}La_2$ and Mg_3La at −1.9 V, and $Mg_{17}La_2$, Mg_3La, and MgLa at −1.95 V vs. Ag/Ag^+ [58]. $Mg_{24}Tm_5$ forms in LiCl–KCl–$TmCl_3$ melts at 923 K through galvanostatic electrolysis at −5.94 A/cm^2 [59]. Meanwhile, Mg_2Tm can be identified by X-ray diffraction (XRD) when the Tm concentration is increased by 6wt%. For the preparation of Mg–Yb alloy, only Mg_2Yb is formed in LiCl–KCl–$YbCl_3$ melts at 743 K by potentiostatic electrolysis at −1.8 and −2.5 V vs. Ag/Ag^+ [60]. Hua *et al.* [61] studied the recovery of Nd from NdFeB magnets in $MgCl_2$–KCl melts and found that Nd can be extracted by reacting with $MgCl_2$.

2.2.3. Al electrode

Electrochemical extraction of REEs on Al electrode was extensively investigated. However, few studies used Al electrode to separate REEs. Many studies have focused on the electrochemical formation and phase control of Al–RE alloy. This section reviews the electrochemical recovery of REEs on the reactive Al electrode in molten salts.

Ji *et al.* [62] reported the separation of La from Sm on solid Al electrode in LiCl–KCl–$LaCl_3$–$SmCl_3$ melts at 773 K. In this case, the recovery efficiency of La was estimated to be 99.1% by potentiostatic electrolysis at −1.45 V vs. Ag/Ag^+ for 40 h. Liu *et al.* [63] studied the electroextraction of Sm in LiCl–KCl–$AlCl_3$–Sm_2O_3 melts at 773 K, in which the extraction efficiencies reached 88.7% at −1.7 V vs. Ag/Ag^+ for 26 h and 94% at −40 mA for 22 h. Similarly, the extraction efficiencies of Gd on the Al electrode at 773 K are 89.7% at −1.5

V vs. Ag/Ag^+ for 26 h and 96.5% at −30 mA for 24 h [64]. Table 1 lists the electrochemical formation and phase control of Al–RE alloy in the LiCl–KCl system [65−86]. Different intermetallic compounds are obtained because the phase

Table 1. Electrochemical formation and phase control of Al–RE alloy in the LiCl–KCl system

Rare earth metals	Temperature / K	Applied current / potential	Intermetallic compound
Sc [65]	723	–1.7 V	Al_3Sc
		–1.95 V	Al_3Sc, Al_2Sc
		–100 mA	Al_3Sc
		–175 mA	Al_3Sc, Al_2Sc, $AlSc_2$
La [62]	773	–1.45 V	$Al_{11}La$, $Al_{2.12}La_{0.88}$
La [66]	723	–1.55 V	$Al_{11}La$
Ce [67]	773	–1.6 V	$Al_{11}Ce$
		–1.9 V	$Al_{11}Ce$, Al_3Ce
		–2.1 V	Al_3Ce, Al_2Ce, AlCe
Ce [68]	873	–1.7 V	Al_4Ce
Pr [69]	723	–1.95 V	Al_2Pr
Pr [70]	723	–3.08 V vs. Cl_2/Cl^-	$Al_{11}Pr_3$
Sm [38]	773	–1.7 V	Al_3Sm
Sm [71]	723	–2.15 to –2.25 V	Al_3Sm
		–2.25 to –2.45 V	Al_3Sm, Al_2Sm
Sm [63]	773	–1.75 V	Al_3Sm
		–2.0 V	Al_3Sm
		–40 mA	Al_3Sm, Al_4Sm
Sm [72]	773	–1.8 V	Al_3Sm
		–2.1 V	Al_3Sm, Al_2Sm
Eu [73]	723	–2.45 V	Al_4Eu
Gd [74]	723	–1.9 V	Al_3Gd
		–2.3 V	Al_3Gd, Al_2Gd
Gd [64]	773	–1.5 V	Al_3Gd
		–2.0 V	Al_3Gd
		–30 mA	Al_3Gd, Al_2Gd, AlGd
Tb [75]	773	–1.8 V	Al_2Tb
	823	–1.9 V	Al_2Tb
Dy [76]	723	–2.98 V vs. Cl_2/Cl^-	Al_3Dy
Dy [77]	773	–1.5 V	Al_3Dy
		–1.6 V	Al_3Dy
		–50 mA	Al_3Dy, AlDy
Ho [78]	723	–1.8 to –2.2 V	Al_3Ho
		–2.35 to –2.4 V	Al_2Ho
		–2.5 V	Al_3Ho, Al_2Ho
Ho [79]	773	–1.5 V	$Al_{17}Ho_2$, Al_3Ho
		–1.8 V	$Al_{17}Ho_2$, Al_3Ho
		–2.0 V	Al_3Ho, Al_2Ho
		–2.2 V	Al_3Ho, Al_2Ho
Er [80]	723	–3.08 V vs. Cl_2/Cl^-	Al_3Er
Er [81]	773	–1.6 V	Al_3Er
		–30 mA	Al_3Er, Al_2Er
Tm [82]	723	–1.9 to –2.1 V	Al_3Tm, Al_2Tm
		–2.3 to –2.45 V	Al_3Tm, Al_2Tm, AlTm
Tm [83]	753	–1.9 V	Al_3Tm, Al_2Tm
		–2.2 V	Al_3Tm, Al_2Tm
		–2.3 V	Al_3Tm, Al_2Tm, AlTm
Yb [84]	723	–2.3 V	Al_3Yb
		–2.4 V	Al_3Yb, Al_2Yb
Yb [85]	753	–2.2 V	Al_3Yb
		–2.3 V	Al_3Yb, Al_2Yb
Lu [86]	723	–2.0 V	Al_3Lu
		–2.35 V	Al_3Lu, Al_2Lu

Note: The potential is versus Ag/AgCl unless otherwise specified.

composition is affected by various experimental parameters, such as temperature, electrolysis time, and metal ion concentration. Therefore, the formation mechanism of Al–RE alloy is different from that of Ni–RE alloy. For Ni–RE alloy, the Ni_2RE alloy phase rapidly forms under different experiment conditions. Nevertheless, Al in RE-rich alloy phase can be obtained under a relatively negative applied potential.

For the Al–Nd alloy phase, the electroextraction of Nd was investigated in NaCl–KCl melts at 1003 K, and the AlNd, $AlNd_2$, and $AlNd_3$ phases were obtained by galvanostatic electrolysis at –0.6 A [87]. On the basis of the obtained results of REE alloy phases on Al electrode in Table 1, Al_3RE is easily formed for Sc, Sm, Gd, Dy, Ho, Er, Tm, Yb, and Lu, and the elements in $Al_{11}RE_3$ correspond to La and Ce.

2.2.4. Fe electrode

Fe as an electrode could be used to produce Fe–Nd alloys in LiF–NdF_3 melts at 1173 K, and one of its important applications is the Nd–Fe–B magnets [88]. Fe_2Dy alloy is usually used as a giant magnetostrictive material [89]. Konishi *et al.* [90] studied the electrochemical process of Fe–Dy alloy in LiCl–KCl–$DyCl_3$ melts at 773 K and found that Fe_2Dy and $Fe_{23}Dy_6$ could be formed through potentiostatic electrolysis at 0.55 and 0.68 V vs. Li/Li^+. For the recovery of REEs from magnet scraps, the electrochemical deposition of Fe–Dy and Fe–Nd alloys was investigated in $CaCl_2$–LiCl melts at 873 K [91]. In this case, $Fe_{17}Nd_2$ and Fe_5Dy were obtained by potentiostatic electrolysis at 0.3 and 0.5 V vs. Li/Li^+ in $CaCl_2$–LiCl–$NdCl_3$ and $CaCl_2$–LiCl–$DyCl_3$ melts, respectively.

2.2.5. Co electrode

Co–RE alloy has attracted considerable interest because of its broad range of magnetic properties. Iida *et al.* [92] prepared Co–Sm alloy in LiCl–KCl melts and found that Sm_2Co_{17}, $SmCo_3$, and $SmCo_2$ could be formed through the anodic potentiostatic electrolysis of $Li_xSm_4Co_6$ at 1.4, 0.8, and 0.3 V vs. Li/Li^+, respectively. Using the same method, Kubota *et al.* [93] found that $CoGd_3$, Co_2Gd, and Co_7Gd_2 could be obtained at 0.55, 0.8, and 0.96 V vs. Li/Li^+, respectively.

2.2.6. Cu electrode

The active Cu could be also employed as an electrode to recover and separate REEs in the LiCl–KCl system. Konishi *et al.* [94] investigated the separation of Dy from Nd in LiCl–KCl–$NdCl_3$–$DyCl_3$ melts at 723 K. In this study, the mass ratios of Dy/Nd in the alloy sample ranged from 6 to 12. In this case, Cu_2Dy could be rapidly formed on a Cu plate electrode. The relationship between Cu_2Dy thickness (h) and electrolysis time (t) is almost parabolic as $h = 10\sqrt{t}$, and the growth rate is approximately 5 μm/h, which is lower than that of Ni_2Dy (28 μm/h).

The electrochemical extraction of REEs on Cu electrode was performed in the LiCl–KCl–$RECl_3$ system [95−101]. Fig. 6(a) shows a series of square wave voltammograms of Ho(III) on W electrode in LiCl–KCl melts at 773 K. The reduction peak of Ho(III) gradually disappears as the electrolysis time is prolonged. ICP–AES revealed that the maximum extraction efficiency is 99.37%, as displayed in Fig. 6(b). The extraction efficiencies of other REEs were also investigated on Cu electrode in the LiCl–KCl–$RECl_3$ system. The extraction efficiencies and electrolysis conditions are listed in Table 2. The extraction efficiencies of most REEs are ≥99%, indicating that using Cu electrode for REE recovery has great potential. In addition, CuRE, Cu_2RE, and Cu_5RE are the main alloy phases during electrolysis.

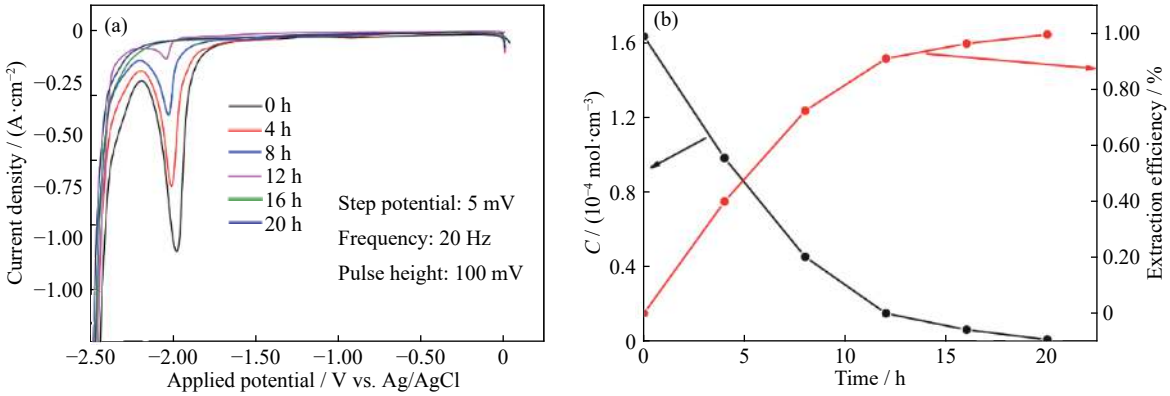

Fig. 6. (a) Square wave voltammograms obtained on W electrode after potentiostatic electrolysis using Cu electrode at −2.15 V vs. Ag/Ag^+ in LiCl–KCl–$HoCl_3$ melts at 773 K; (b) Change in Ho ion concentration (C) and extraction efficiency along with electrolysis time. Reprinted from W. Han, Z.Y. Li, M. Li, X. Hu, X.G. Yang, M.L. Zhang, and Y. Sun, Journal of The Electrochemical Society, 164, D934-D943(2017) [96]. © IOP Publishing. Reproduced with permission. All rights reserved.

2.3. Electroextraction by alloying on liquid electrode

2.3.1. Sn electrode

According to the principle of separation shown in Fig. 2, the separation and recovery of Dy and Nd metals were investigated on liquid Sn electrode in LiCl–KCl–$DyCl_3$–$NdCl_3$ melts at 723 K [29]. The separation of Nd from Dy could be easily achieved to form Sn–Nd alloy because of the large dif-

Table 2. Extraction efficiencies of rare earth metals obtained on Cu electrode

Rare earth metals	Applied current density / potential	Temperature / K	Intermetallic compound	Extraction efficiency / %
Pr [100]	–2.2 V	823	CuPr	99.81
Sm [38]	–1.6 V	773	Cu_6Sm	—
Gd [101]	–2.2 V	823	CuGd, Cu_2Gd	99.6
Tb [99]	31 mA/cm^2	773	CuTb, Cu_2Tb	97.7
Dy [98]	–2.15 V	773	CuDy, Cu_2Dy	99.2
Ho [96]	–2.15 V	773	Cu_2Ho, Cu_5Ho	99.37
Er [97]	–2.2 V	823	CuEr	98.92
Yb [95]	–2.3 V	803	Cu_2Yb, Cu_5Yb	99.9

Note: The potential is versus Ag/AgCl.

ference in deposition potential between Nd and Dy. The mass ratio of Nd/Dy in the alloy sample was identified to be 3.11 by potentiostatic electrolysis at 0.6 and 0.7 V vs. Li/Li$^+$, which is much lower than that (72) obtained on a Ni-based alloy diaphragm [43]. The liquid Sn electrode was employed to separate Nd from Dy, whereas Ni electrode is just the opposite for the separation of Dy from Nd.

2.3.2. Zn electrode

Zn metal as a solid electrode was introduced to study the electrochemical separation of Dy and Nd in LiCl–KCl–$DyCl_3$–$NdCl_3$ melts at 653 K [28]. The reduction potential of Nd on solid Zn electrode is more positive than that of Dy. In this case, Nd could be first extracted as the Zn–Nd alloy by potentiostatic electrolysis at an applied potential of 0.8–1.2 V vs. Li/Li$^+$. The highest mass ratio of Nd/Dy was identified to be 3.3 at 1.0 V vs. Li/Li$^+$.

The recovery of REEs was extensively studied using liquid Zn electrode, whereas the separation of REEs as individual metals was rarely investigated in this system. The extraction of REEs and the extraction efficiency are summarized in Table 3. Kamimoto *et al.* [102−104] investigated the recovery of REEs from magnet scrap leaching solution on the liquid Zn electrode. In this process, REEs were first leached from the boundary phase of magnets by using potentiostatic electrolysis in LiCl–KCl melts at −1.0 V vs. Ag/Ag$^+$. Simultaneously, REE recovery can be achieved on the liquid Zn electrode. The mass content of REEs in the electrodeposit was found to be ≥99.8%, and the current efficiency was calculated to be 91.5%. Han *et al.* [105] extracted Y by using the liquid Zn electrode and obtained extraction efficiencies of 95.8% and 91.5% through galvanostatic electrolysis at −0.15 A and potentiostatic electrolysis at −1.4 V vs. Ag/Ag$^+$, respectively. Li *et al.* [99] further studied Tb extraction and estimated the extraction efficiency to be 90.6% via galvanostatic electrolysis at −31 mA/cm^2. Liu *et al.* [106] performed the electrochemical extraction of Sm LiCl–KCl–$SmCl_3$ melts by potentiostatic electrolysis at −2.4 V vs. Ag/Ag$^+$ and determined the extraction efficiency to be 94.5%. For the recovery of other REEs on the liquid Zn electrode, the feasibility of extraction was manifested, but the extraction efficiencies were not reported [107−113].

2.3.3. Ga electrode

Gallium has the lowest melting point of the post-transition metals. Hence, it was also employed to investigate the

Table 3. Extraction efficiencies of rare earth metals obtained on liquid Zn electrode

Rare earth metal	Temperature / K	Applied current density / potential	Intermetallic compound	Extraction efficiency / %
Y [105]	823	–0.15 A	$Zn_{12}Y$	95.8
	823	–1.4 V	$Zn_{12}Y$	89.7
Ce [107]	723	–1.4 V	$Zn_{11}Ce$	—
Pr [108]	773	–96.8 mA/cm^2	$Zn_{11}Pr$, $Zn_{17}Pr_2$, $Zn_{58}Pr_{13}$, $Zn_{11}Pr_3$, ZnPr	—
Nd [109]	751	–1.6 V	$Zn_{12}Nd_2$	—
Sm [38]	773	–150 mA/cm^2	$Zn_{17}Sm_2$	—
Sm [106]	873	–1.6 V	$Zn_{12}Sm$, $Zn_{17}Sm_2$	—
	873	–2.4 V	$Zn_{17}Sm_2$	94.5
Gd [110]	773	–1.34 V	$Zn_{12}Gd$	—
Tb [99]	773	–31 mA/cm^2	$Zn_{17}Tb_2$	90.6
Ho [111]	843	–1.4 V	$Zn_{17}Ho_2$	—
Tm [112]	753	–0.2 A/cm^2	$Zn_{17}Tm_2$	—
Yb [113]	813	–0.8 A	$Zn_{11}Yb$, Zn_2Yb, $Zn_{11}Yb_3$	—

Note: The potential is versus Ag/AgCl.

recovery of REEs in molten salts. The electrochemical behaviors and electroextraction of La, Ce, Nd, and Gd were investigated in LiCl–KCl melts by using liquid Ga electrode [114−116]. La(III) ion was extracted as Ga_6La by potentiostatic electrolysis at −1.37 V vs. Ag/Ag^+ in LiCl–KCl–$LaCl_3$ melts. Different currents were applied to extract Ce metal in LiCl–KCl–$CeCl_3$ melts at 723 K. In this study, Ga_6Ce was identified by XRD, and the ICP results showed that the current efficiency is about 90%. A galvanostatic electrolysis at −10 mA was conducted to recover Nd and Gd as Ga_6Nd and Ga_6Gd in LiCl–KCl–$NdCl_3$ and LiCl–KCl–$GdCl_3$ melts, respectively. Table 4 shows the Ga–RE intermetallic compounds obtained on liquid Ga electrode at different conditions. Ga_6RE is the main alloy phase under the conditions of potentiostatic or galvanostatic electrolysis.

2.3.4. Bi electrode

The electrochemical extraction of REEs was studied using liquid Bi electrode in LiCl−KCl melts [117−121]. Table 5 shows the Bi–RE alloy phase at different experimental conditions. The BiRE phase easily forms under the conditions of potentiostatic or galvanostatic electrolysis. In the study of Ho extraction, the relationship between extraction efficiency and electrolysis time was illustrated, and the maximum extraction efficiency was identified to be 95.9% via potentiostatic electrolysis at −1.6 V vs. Ag/Ag^+. For other REEs on liquid Bi electrode, the extraction efficiency was not mentioned in the reported literature.

2.4. Summary of separation/recovery of REEs

The separation of REEs at different electrodes was discussed above. The research targets include Pr, Nd, Dy, and Tb. Table 6 summarizes the separation of the REEs in detail. REE separation using a solid electrode is better than that using a liquid electrode, and the high separation factor is determined on Ni electrode. In addition, LiCl–KCl melts are more suitable for the separation of REEs than NaCl–KCl and LiF–CaF_2 systems. Basing from the research of "bifunctional" electrode for the separation of REEs, Ito *et al.* [122] simulated the extraction and separation of REEs. The simulation process shows less iterative operations and requires high purity. However, the processes have not been commercialized because of the high process cost and unstable price of REEs [123].

Electrochemical alloying/dealloying was reviewed on solid and liquid electrodes. The formation of intermetallic compounds could be related to experimental conditions (temperature, ions concentration, electrolysis parameter, and electrolysis technique) and thermodynamic and kinetic properties. After comparison of the 10 electrodes, some properties can be summarized below.

(1) The alloy phase Ni_2RE forms more easily than other Ni–RE intermetallic compounds regardless of electrolysis condition and electrolyte (chloride and fluoride melt), which is ascribed to the high RE diffusivity in and near the grain boundaries. Although the studies of REEs on Co and Cu electrodes obtained the same result with Ni, few REEs were included. For solid Al electrode, the types of Al–RE alloy phase are strongly affected by electrolysis conditions.

(2) When REEs are electrodeposited on a liquid electrode, RE metals are first dissolved in the liquid electrode. After the

Table 4. Ga–RE intermetallic compounds obtained on liquid Bi electrode at different conditions

Rare earth metals	Temperature / K	Applied current density/potential	Intermetallic compound
La [114]	723	–1.37 V	Ga_6La
Ce [115]	723	–18.57 to –39.78 mA/cm^2	Ga_6Ce
Nd [115]	723	–26.53 mA/cm^2	Ga_6Nd
Gd [116]	673	–8.85 mA/cm^2	Ga_6Gd

Note: The potential is versus Ag/AgCl.

Table 5. Bi–RE intermetallic compounds using liquid Bi electrode at different conditions

Rare earth metals	Applied current density / potential	Temperature / K	Intermetallic compound
Y [117]	–32.79 to –163.93 mA/cm^2	773	BiY
La [118]	–63.4 mA/cm^2	773	Bi_2La, BiLa
	–1.4 V	773	Bi_2La, BiLa, $BiLa_2$
Ho [119]	–1.5 V	773	BiHo
	–32.3 mA/cm^2	773	BiHo
Tb [120]	–100 mA/cm^2	773	TbBi
	–250 mA/cm^2	773	TbBi
	–1.55 V	773	TbBi, Tb_5Bi_3, Tb_4Bi_3
Dy [121]	–64.5 mA/cm^2	773	BiDy
	–12.9 mA/cm^2	773	BiDy

Note: The potential is versus Ag/AgCl.

Table 6. Summary of separation REEs on different systems

System	Electrode	Electrolysis condition	Temperature / K	Separation REEs	Mass ratio
LiCl–KCl–$TbCl_3$–$NdCl_3$	Ni	0.7 V vs. Li/Li^+	723	Tb/Nd	56
LiCl–KCl–$DyCl_3$–$NdCl_3$	Ni	0.65 V vs. Li/Li^+	723	Dy/Nd	72
LiCl–KCl–$DyCl_3$–$NdCl_3$–$PrCl_3$	Ni	0.65 V vs. Li/Li^+	723	Dy/(Nd+Pr)	50
LiCl–KCl–(Nd magnet)Cl_n	Ni	0.67 V vs. Li/Li^+	723	Dy/Nd	30
NaCl–KCl–$DyCl_3$–$NdCl_3$–$PrCl_3$	Ni	0.42 V vs. Na/Na^+	973	Dy/(Nd+Pr)	9.9
		0.45 V vs. Na/Na^+	973	Dy/(Nd+Pr)	22.9
LiF–CaF_2–NdF_3–DyF_3	Ni	0.34−0.40 V vs. Li/Li^+	1123	Dy/Nd	5.6
LiCl–KCl–$DyCl_3$–$NdCl_3$	Cu	0.45−0.75 V vs. Li/Li^+	723	Dy/Nd	6−12
LiCl–KCl–$DyCl_3$–$NdCl_3$	Sn	0.6 and 0.7 V vs. Li/Li^+	723	Nd/Dy	3.11
LiCl–KCl–$DyCl_3$–$NdCl_3$	Zn	1.0 V vs. Li/Li^+	653	Nd/Dy	3.3

saturation of RE in the liquid electrode, intermetallic compounds are produced. Therefore, the M–richest alloy phase could first be formed during alloying on a liquid electrode. Moreover, the high extraction efficiency of REEs on the liquid electrode could be determined.

(3) On the basis of the results of electrochemical alloying and dealloying, a large number of fundamental data for the preparation of RE–transition metal alloys were determined, which might provide support for practical applications.

(4) The electrochemical separation on the solid electrode was determined by the different growth rates and potential difference. However, REEs have a close potential difference on liquid electrodes. Hence, the separation factor is lower than that on the solid electrode. Due to the fluidity of liquid metal and the solubility of REEs, the liquid electrode could satisfy the recovery of REEs in practical applications.

3. Thermodynamic evaluation of the feasibility of FLiNaK electrolyte for REE recovery

On the basis of thermodynamic calculation, the recovery of REEs from magnet scraps was performed through selective chlorination using different chlorinating agents. Itoh *et al.* [124] recovered $NdCl_3$ from NdFeB magnets by using NH_4Cl as the chlorination reagent. Uda [8] extracted 96% Nd and 94% Dy in magnet scraps into chloride phase by chlorination with $FeCl_2$. Shirayama and Okabe [125] recovered at most 87% Nd and 78% Dy in NdFeB magnet scraps by utilizing molten $MgCl_2$. Then, Hua *et al.* [61] extracted more than 90% REEs in magnet scraps by using molten $MgCl_2$–KCl salt and produced Mg–RE alloy directly through molten salt electrolysis in this system. In the production of RE metals, the fluoride system is favored over the chloride system because of the low current efficiencies, evolution of chlorine gas, and production of low-melting-point REEs in chloride melts [126]. Abbasalizadeh *et al.* [127] studied the selective extraction of REEs in LiF–NdFeB by using AlF_3, ZnF_2, and FeF_3 as the fluorinating agents. To avoid gas release on the anode, Yang *et al.* [128] performed experiments in LiF–CaF_2 melts by using Nd–Pr and NdFeB magnets as the anodic materials, where Nd and Pr were selectively oxidized. Taxil *et al.* studied the electrochemistry of REEs in LiF–CaF_2 melts, such as Nd [51], Sm [129], Eu [130], Gd [53], and Dy [54]. In this study, we evaluated the feasibility of LiF–NaF–KF melts as the electrolyte for the recovery of REEs.

A eutectic mixture LiF–NaF–KF (FLiNaK, 46.5LiF–11.5NaF–42KF, mol%) was proposed as a promising coolant in molten salt reactor applications [131]. Some studies focused on the corrosion of materials and reprocessing fission products in FLiNaK melts. REs are the major fission products in nuclear reactors that need to be separated from the coolant [132]. Hamel *et al.* [133] studied the cathodic process of NdF_3 in LiF–CaF_2, LiF–KF, and LiF–NaF systems, in which LiF–KF and LiF–NaF mixtures are unsuitable to Nd electrowinning because of the oxidation reaction of potassium and sodium ions with Nd metal. However, experimental evidence to support the conclusion is lacking. Zhu [134] evaluated the feasibility of using fluoride electrolyte based on the theoretical decomposition voltage that only LiF, CaF_2, SrF_2, and BaF_2 satisfy the supporting electrolyte for the active rare earth oxide. However, Wang *et al.* [135] proved that La can be separated in FLiNaK melts and corrected the electrochemical study of LaF_3 in FLiNaK melts [136]. On the basis of the discussion above, the thermodynamics of the feasibility of FLiNaK electrolyte for the recovery of REEs was evaluated.

The melting point of different fluoride systems is summarized in Table 7. The FLiNaK system shows the lowest melting point, which is about 455°C [137]. Therefore, the operating temperature using FLiNaK electrolyte is much lower

Table 7. Melting points of different fluoride systems

Fluoride system	Melting point / °C
LiF	846
77mol%LiF–23mol%CaF_2	760
60mol%LiF–40mol%NaF	652
50mol%LiF–50mol%KF	492
46.5mol%LiF–11.5mol%NaF–42mol%KF	455

than that of other fluoride systems.

The standard reduction potentials for REEs in FLiNaK melt were first calculated to confirm the feasibility of using FLiNaK electrolyte. The working temperature was set at 700°C. Pure rare earth fluorides of melting points are above 700°C. Hence, the standard reduction potentials should be calculated at the supercooled liquid salt [138]. Table 8 shows the values in FLiNaK–REF_3 melts at 700°C. Zhu [134] also calculated the theoretical decomposition voltages for fluorides at different temperatures. On the basis of the calculated standard reduction potentials, a coordinate graph is displayed in Fig. 7. Most REEs of standard reduction potentials are negative than NaF/Na and KF/K, which means that the RE metals cannot be obtained in the FLiNaK system.

Table 8. Calculated standard reduction potentials of LiF/Li, NaF/Na, KF/K, CaF_2/Ca, and REF_3/RE at 700°C

Redox couple	Standard reduction potential, $E^{\ominus}$ / V vs. F_2/F^-
LiF/Li	–5.381
NaF/Na	–4.848
KF/K	–4.827
CaF_2/Ca	–5.440
LaF_3/La	–5.007
CeF_3/Ce	–4.928
PrF_3/Pr	–4.934
NdF_3/Nd	–4.934
GdF_3/Gd	–4.976
DyF_3/Dy	–4.954
HoF_3/Ho	–4.958
ErF_3/Er	–4.961
TmF_3/Tm	–4.332
ScF_3/Sc	–4.673
YF_3/Y	–4.760

The result is the same as that in the study by Hamel *et al.* [133], in which the deposited Nd metal was oxidized by KF or NaF electrolyte. Therefore, when the RE metals are oxidized by KF or NaF, the reaction can be expressed as follows:

$$3NaF + RE = 3Na + REF_3 \quad (3)$$

$$3KF + RE = 3K + REF_3 \quad (4)$$

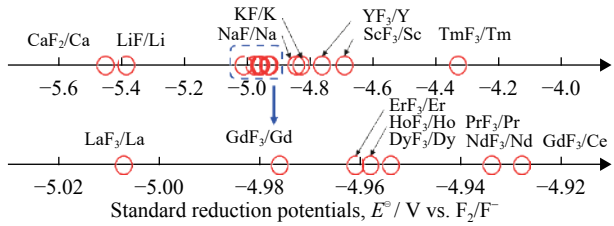

Fig. 7. Coordinate graph of standard reduction potentials of LiF/Li, NaF/Na, KF/K, CaF_2/Ca, and REF_3/RE at 700°C.

Fig. 8 shows the relationship between the standard Gibbs free energy of reactions and temperature, which were calculated by HSC chemistry 6.0 [139]. The results indicate that reactions (3) and (4) are very close. The values of Tm, Eu, Yb, and Sc are higher than zero at the temperature range of 500–1200°C. The value of Er is around zero. Other values of REEs are less than zero, indicating that the reactions are spontaneous.

According to the thermodynamic evaluation above, the FLiNaK electrolyte cannot satisfy the requirement for REE recovery. However, some new studies showed good results for supporting REE separation in the FLiNaK system. Wang *et al.* [135] separated La metal on inert tungsten and molybdenum electrodes via electrochemistry in FLiNaK melts, which corrected the previous study [136], as shown in Fig. 9. La metal can also be electrodeposited in LiF–KF and LiF–NaF systems [140]. Some studies showed that La exists in the species of LaF_6^{3-} instead of La^{3+} when dissolved in fluoride melt containing KF or NaF. Therefore, reactions (3) and (4) are unsuitable to calculate the thermodynamic data. The standard reduction potential of K_3LaF_6/La was calculated to be −3.97 V, which is about 1.04 V more positive than that of LaF_3/La [140]. Therefore, the addition of KF or NaF assists the extraction of La metal. Constantin *et al.* [141−142]

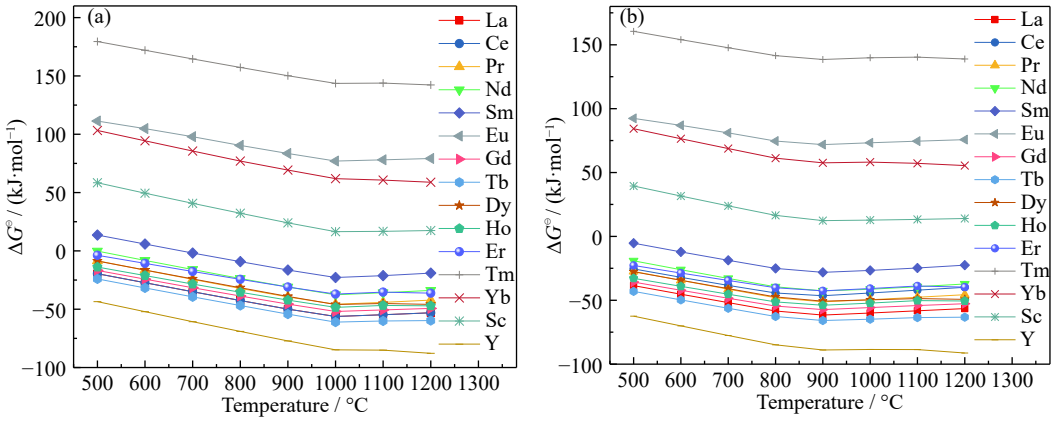

Fig. 8. Relationship between the standard Gibbs free energy of (a) reaction (3) and (b) reaction (4) with temperature.

studied the electrochemistry of Ce in fluoride melt, in which Ce metal of 99.5% purity (determined by XRD) was obtained. When CeF_3 was added in LiF–NaF melts, Ce existed in the species of $NaCeF_4$ instead of CeF_3. The binary phase diagram of alkali metal fluorides and REF_3 shows that almost all REEs form xKF·yREF$_3$ or xNaF·yREF$_3$ stoichiometric compounds [143−145]. However, few studies are correlated with the thermodynamic data and electrochemical experiments. Multicomponent phase diagrams, including the ratio of REF_3, in eutectic FLiNaK are a major concern in REE recovery. Therefore, FLiNaK electrolyte has a great potential for alternative research to recover REEs.

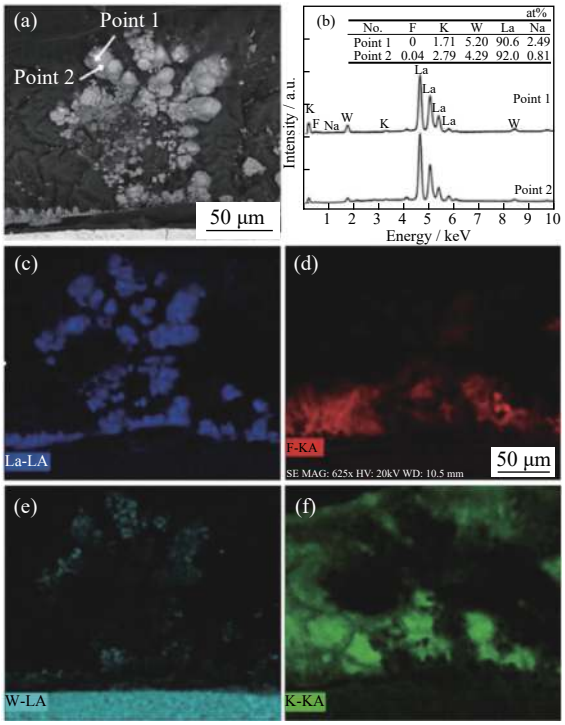

Fig. 9. SEM results of the deposit after chronopotentiometry electrolysis in FLiNaK–LaF_3 melts. Reprinted from *J. Nucl. Mater.*, 518, Y.F. Wang, J.B. Ge, W.Q. Zhuo, S.Q. Guo, and J.S. Zhang, Electrochemical separation study of LaF_3 in molten FLiNaK salt, 162-165, Copyright 2019, with permission from Elsevier.

4. Conclusions

This review summarizes the electrochemical separation and recovery of REEs on reactive solid and liquid electrodes in molten salts. The electrochemical separation on a solid electrode was determined by the different growth rates and potential differences. REE separation using a solid electrode is better than that using a liquid electrode, and the high separation factor is determined on Ni electrode. The alloy phase Ni_2RE forms more easily than other Ni–RE intermetallic compounds regardless of electrolysis condition and electrolyte (chloride and fluoride melt), which is ascribed to the high RE diffusivity in and near the grain boundaries. In addition, the LiCl–KCl eutectic salt is more suitable for the separation process than other electrolytes, such as NaCl–KCl and LiF–CaF_2 melts.

On the basis of electrochemical alloying and dealloying, fundamental data for the preparation of RE–transition metal alloys were determined. The relationship between the applied potential/current and types of alloy phase was discussed. A high extraction efficiency of 95%–99% could be achieved. Due to the fluidity of liquid metal and the solubility of REEs, the liquid electrode could satisfy the recovery of REEs in practical applications. Although considerable progress has been achieved in the electroseparation from molten salt, further consideration for practical applications is lacking in the published literature. Some critical challenges should be considered. The design of operation cell is limited for practical applications. Molten salt exhibits volatility and strong corrosivity under high experimental temperatures, which requires an ideal cell material for conducting a long time.

Considering the results of this review, we recommend FLiNaK salt as the electrolyte for REE recovery. REEs exist in the species of REF_6^{3-} instead of RE^{3+} when dissolved in FLiNaK melts. On the basis of the thermodynamic evaluation of REEs in FLiNaK melts, the conclusion that potassium and sodium ions oxidize the deposited neodymium might be untenable. Interestingly, the addition of KF or NaF assists the extraction of RE metal. In addition, the price of lithium compound increases with the growing lithium demand in batteries. Hence, adding KF and NaF would reduce the cost. Although the production of REEs has increased remarkably, reducing the energy consumption for electrolysis is still the major future direction because of the low current efficiency and high cell voltage currently. Ternary FLiNaK melts show a lower melting point than other binary melts. Hence, the energy consumption will be reduced in this system. Fundamental studies including electrochemistry, thermodynamic calculation, and extraction efficiency are still warranted.

Acknowledgements

This work was supported by the National Natural Science Foundation of China (Nos. 21976047, 21790373, and 51774104), the Ph.D Student Research and Innovation Fund of the Fundamental Research Funds for the Central Universities (No. 3072019GIP1011), University and Local Integration Development Project of Yantai, China (No. 2020 XDRHXMPT36), and the Sino-Russian Cooperation Fund of Harbin Engineering University (No. 2021HEUCRF004).

References

[1] Y.X. Yang, A. Walton, R. Sheridan, K. Güth, R. Gauß, O.

Gutfleisch, M. Buchert, B.M. Steenari, T. Van Gerven, P.T. Jones, and K. Binnemans, REE recovery from end-of-life Nd-FeB permanent magnet scrap: A critical review, *J. Sustainable Metall.*, 3(2017), No. 1, p. 122.

[2] M. Tanaka, T. Oki, K. Koyama, H. Narita, and T. Oishi, Recycling of rare earths from scrap, *Handb. Phys. Chem. Rare Earths*, 43(2013), p. 159.

[3] K.M. Goodenough, F. Wall, and D. Merriman, The rare earth elements: demand, global resources, and challenges for resourcing future generations, *Nat. Resour. Res.*, 27(2018), No. 2, p. 201.

[4] J.P. Rabatho, W. Tongamp, Y. Takasaki, K. Haga, and A. Shibayama, Recovery of Nd and Dy from rare earth magnetic waste sludge by hydrometallurgical process, *J. Mater. Cycles Waste Manage.*, 15(2013), No. 2, p. 171.

[5] M. Firdaus, M.A. Rhamdhani, Y. Durandet, W.J. Rankin, and K. McGregor, Review of high-temperature recovery of rare earth (Nd/Dy) from magnet waste, *J. Sustain. Metall.*, 2(2016), No. 4, p. 276.

[6] K. Murase, K. Machida, and G. Adachi, Recovery of rare metals from scrap of rare earth intermetallic material by chemical vapour transport, *J. Alloys Compd.*, 217(1995), No. 2, p. 218.

[7] T. Uda, K.T. Jacob, and M. Hirasawa, Technique for enhanced rare earth separation, *Science*, 289(2000), No. 5488, p. 2326.

[8] T. Uda, Recovery of rare earths from magnet sludge by $FeCl_2$, *Mater. Trans.*, 43(2002), No. 1, p. 55.

[9] Y.C. Xu, L.S. Chumbley, and F.C. Laabs, Liquid metal extraction of Nd from NdFeB magnet scrap, *J. Mater. Res.*, 15(2000), No. 11, p. 2296.

[10] H. Konishi, T. Nohira, and Y. Ito, Formation and phase control of Dy alloy films by electrochemical implantation and displantation, *J. Electrochem. Soc.*, 148(2001), No. 7, p. C506.

[11] T. Oishi, H. Konishi, T. Nohira, M. Tanaka, and T. Usui, Separation and recovery of rare earth metals by molten salt electrolysis using alloy diaphragm, *Kagaku Kogaku Ronbunshu*, 36(2010), No. 4, p. 299.

[12] S. Kobayashi, K. Kobayashi, T. Nohira, R. Hagiwara, T. Oishi, and H. Konishi, Electrochemical formation of Nd−Ni alloys in molten $LiF-CaF_2-NdF_3$, *J. Electrochem. Soc.*, 158(2011), No. 12, p. E142.

[13] D.H. Tian, Z.C. Han, M.Y. Wang, and S.Q. Jiao, Direct electrochemical N-doping to carbon paper in molten $LiCl-KCl-Li_3N$, *Int. J. Miner. Metall. Mater.*, 27(2020), No. 12, p. 1687.

[14] Y.H. Liu, M. Tang, S. Zhang, Y.L. Lin, Y.C. Wang, Y.Q. Wang, Y. Dai, X.H. Cao, Z.B. Zhang, and Y.H. Liu, Insights into U(VI) adsorption behavior onto polypyrrole coated 3R-MoS_2 nanosheets prepared with the molten salt electrolysis method, *Int. J. Miner. Metall. Mater*, (2020). DOI: 10.1007/s12613-020-2154-5

[15] X.X. Liang, J.X. Xiao, W. Weng, and W. Xiao, Electrochemical reduction of carbon dioxide and iron oxide in molten salts to Fe/Fe_3C modified carbon for electrocatalytic oxygen evolution, *Angew. Chem. Int. Ed.*, 60(2021), No. 4, p. 2120.

[16] T. Lv, J.X. Xiao, W. Weng, and W. Xiao, Electrochemical fixation of carbon dioxide in molten salts on liquid zinc cathode to zinc@graphitic carbon spheres for enhanced energy storage, *Adv. Energy Mater.*, 10(2020), No. 39, p. 2002241.

[17] W. Weng, S.B. Wang, W. Xiao, and X.W. Lou, Direct conversion of rice husks to nanostructured SiC/C for CO_2 photoreduction, *Adv. Mater.*, 32(2020), No. 29, p. 2001560.

[18] W. Weng, B. Jiang, Z. Wang, and W. Xiao, *In situ* electrochemical conversion of CO_2 in molten salts to advanced energy materials with reduced carbon emissions, *Sci. Adv.*, 6(2020), No. 9, p. 9278.

[19] S.Q. Jiao, H.D. Jiao, W.L. Song, M.Y. Wang, and J.G. Tu, A review on liquid metals as cathodes for molten salt/oxide electrolysis, *Int. J. Miner. Metall. Mater.*, 27(2020), No. 12, p. 1588.

[20] S.M. Chen, C.F. Liao, J.Y. Lin, B.Q. Cai, X. Wang, and Y.F. Jiao, Electrical conductivity of molten $LiF–DyF_3–Dy_2O_3–Cu_2O$ system for Dy–Cu intermediate alloy production, *Int. J. Miner. Metall. Mater.*, 26(2019), No. 6, p. 701.

[21] Y.K. Zhong, K. Liu, Y.L. Liu, Y.X. Lu, T.Q. Yin, L. Wang, Z.F. Chai, and W.Q. Shi, Preparation of γ-uranium-molybdenum alloys by electrochemical reduction of solid oxides in LiCl molten salt, *J. Electrochem. Soc.*, 166(2019), No. 8, p. 276.

[22] D.Y. Zhang, X. Ma, H.W. Xie, X. Chen, J.K. Qu, Q.S. Song, and H.Y. Yin, Electrochemical derusting in molten $Na_2CO_3–K_2CO_3$, *Int. J. Miner. Metall. Mater.*, 28(2021), No. 4, p. 637.

[23] K.L. Nash, and M. Nilsson, Introduction to the reprocessing and recycling of spent nuclear fuels, [in] R. Taylor, ed., *Reprocessing and Recycling of Spent Nuclear Fuel*, Woodhead Publishing, Oxford, 2015, p. 3.

[24] J.J. Laidler, J.E. Battles, W.E. Miller, J.P. Ackerman, and E.L. Carls, Development of pyroprocessing technology, *Prog. Nucl. Energy*, 31(1997), No. 1-2, p. 131.

[25] T. Koyama, Y. Sakamura, M. Iizuka, T. Kato, T. Murakami, and J.P. Glatz, Development of pyro-processing fuel cycle technology for closing actinide cycle, *Procedia Chem.*, 7(2012), p. 772.

[26] A. Novoselova, and V. Smolenski, The influence of the temperature and Ga−In alloy composition on the separation of uranium from neodymium in molten Ga−In/3LiCl−2KCl system during the recycling of high-level waste, *J. Nucl. Mater.*, 509(2018), p. 313.

[27] J.H. Lan, S.L. Jiang, Y.L. Liu, X.M. Yin, Y.X. Wang, T.Q. Yin, S.A. Wang, C.Z. Wang, W.Q. Shi, and Z.F. Chai, Separation of actinides from lanthanides associated with spent nuclear fuel reprocessing in China: current status and future perspectives, *Radiochim. Acta*, 107(2019), No. 9-11, p. 951.

[28] H. Konishi, H. Ono, E. Takeuchi, T. Nohira, and T. Oishi, Electrochemical formation of RE−Zn (RE = Dy, Nd) alloys in a molten LiCl−KCl system, *ECS Trans.*, 61(2014), No. 28, p. 19.

[29] A. Kuriyama, K. Hosokawa, H. Konishi, H. Ono, E. Takeuchi, T. Nohira, and T. Oishi, Electrochemical formation of RE−Sn (RE = Dy, Nd) alloys using liquid Sn electrodes in a molten LiCl-KCl system, *ECS Trans.*, 75(2016), No. 15, p. 341.

[30] P. Souček and R. Malmbeck, Pyrochemical processes for recovery of actinides from spent nuclear fuels, [in] R. Taylor, ed., *Reprocessing and Recycling of Spent Nuclear Fuel*, Woodhead Publishing, Oxford, 2015, p. 437.

[31] P. Taxil, L. Massot, C. Nourry, M. Gibilaro, P. Chamelot, and L. Cassayre, Lanthanides extraction processes in molten fluoride media: Application to nuclear spent fuel reprocessing, *J. Fluorine Chem.*, 130(2009), No. 1, p. 94.

[32] G. Xie, K. Ema, Y. Ito, and M.S. Zhao, Electrochemical formation of Ni−Y intermetallic compound layer in molten chloride, *J. Appl. Electrochem.*, 23(1993), p. 753.

[33] K. Hachiya and Y. Ito, Molecular dynamics simulations of the self-diffusion phenomena in Ni_2Y intermetallic phase, *J. Al-*

loys Compd., 279(1998), No. 2, p. 171.
[34] W. Han, Q. Zhao, J. Wang, M. Li, W.K. Liu, M.L. Zhang, X.G. Yang, and Y. Sun, Electrochemical behavior of Y(III) and preparation of Y−Ni intermetallic compounds in molten LiCl−KCl salts, *J. Rare Earths*, 35(2017), No. 1, p. 90.
[35] T. Nohira, H. Kambara, K. Amezawa, and Y. Ito, Electrochemical formation and phase control of Pr−Ni alloys in a molten LiCl−KCl−$PrCl_3$ system, *J. Electrochem. Soc.*, 152(2005), No. 4, p. C183.
[36] T.Q. Yin, Y. Liang, J.M. Qu, P. Li, R.F. An, Y. Xue, M.L. Zhang, W. Han, G.L. Wang, and Y.D. Yan, Thermodynamic and electrochemical properties of praseodymium and the formation of Ni−Pr intermetallics in LiCl−KCl melts, *J. Electrochem. Soc.*, 164(2017), No. 13, p. D835.
[37] T. Iida, T. Nohira, and Y. Ito, Electrochemical formation of Sm–Ni alloy films in a molten LiCl–KCl–$SmCl_3$ system, *Electrochim. Acta*, 46(2001), No. 16, p. 2537.
[38] T.Q. Yin, L. Chen, Y. Xue, Y.H. Zheng, X.P. Wang, Y. Yongde, M.L. Zhang, G.L. Wang, F. Gao, and M. Qiu, Electrochemical behavior and underpotential deposition of Sm on reactive electrodes (Al, Ni, Cu, and Zn) in a LiCl–KCl melt, *Int. J. Miner. Metall. Mater.*, 27(2020), No. 12, p. 1657.
[39] H. Konishi, K. Mizuma, H. Ono, E. Takeuchi, T. Nohira, and T. Oishi, Electrochemical formation of Tb−Ni alloys in a molten LiCl−KCl−$TbCl_3$ system, *ECS Trans.*, 50(2013), No. 11, p. 561.
[40] H. Konishi, T. Nohira, and Y. Ito, Kinetics of $DyNi_2$ film growth by electrochemical implantation, *Electrochim. Acta*, 48(2003), No. 5, p. 563.
[41] T. Iida, T. Nohira, and Y. Ito, Electrochemical formation of Yb–Ni alloy films by Li codeposition method in a molten LiCl–KCl–$YbCl_3$ system, *Electrochim. Acta*, 48(2003), No. 11, p. 1531.
[42] H. Konishi, H. Ono, T. Oishi, and T. Nohira, Electrochemical formation of Tb alloys in molten LiCl–KCl eutectic melts and separation of Tb, [in] *Proceedings of the TMS Annual Meeting & Exhibition*, 2018, p. 89.
[43] H. Konishi, H. Ono, T. Nohira, and T. Oishi, Separation of Dy and Nd (La) using molten salt and an alloy diaphragm, *ECS Trans.*, 50(2013), No. 11, p. 463.
[44] H. Konishi, H. Ono, E. Takeuchi, T. Nohira, and T. Oishi, Separation of Dy from Nd−Fe−B magnet scraps using molten salt electrolysis, *ECS Trans.*, 64(2014), No. 4, p. 593.
[45] H. Konishi, T. Oishi, T. Nohira, H. Ono, and E. Takeuchi, Dy permeation through an alloy diaphragm using electrochemical implantation and displantation, *ECS Trans.*, 75(2016), No. 15, p. 105.
[46] K. Yasuda, S. Kobayashi, T. Nohira, and R. Hagiwara, Electrochemical formation of Dy–Ni alloys in molten NaCl–KCl–$DyCl_3$, *Electrochim. Acta*, 106(2013), p. 293.
[47] K. Yasuda, S. Kobayashi, T. Nohira, and R. Hagiwara, Electrochemical formation of Nd–Ni alloys in molten NaCl–KCl–$NdCl_3$, *Electrochim. Acta*, 92(2013), p. 349.
[48] K. Yasuda, K. Kondo, T. Nohira, and R. Hagiwara, Electrochemical formation of Pr–Ni alloys in LiF–CaF_2–PrF_3 and NaCl–KCl–$PrCl_3$ melts, *J. Electrochem. Soc.*, 161(2014), No. 7, p. D3097.
[49] K. Yasuda, K. Kondo, S. Kobayashi, T. Nohira, and R. Hagiwara, Selective formation of rare-earth–nickel alloys via electrochemical reactions in NaCl–KCl molten salt, *J. Electrochem. Soc.*, 163(2016), No. 5, p. D140.
[50] S. Kobayashi, T. Nohira, K. Kobayashi, K. Yasuda, R. Hagiwara, T. Oishi, and H. Konishi, Electrochemical formation of Dy-Ni alloys in molten LiF–CaF_2–DyF_3, *J. Electrochem. Soc.*, 159(2012), No. 12, p. E193.
[51] C. Nourry, L. Massot, P. Chamelot, and P. Taxil, Formation of Ni−Nd alloys by Nd(III) electrochemical reduction in molten fluoride, *J. New Mater. Electrochem. Syst.*, 10(2007), No. 2, p. 117.
[52] C. Nourry, L. Massot, P. Chamelot, and P. Taxil, Electrochemical reduction of Gd(III) and Nd(III) on reactive cathode material in molten fluoride media, *J. Appl. Electrochem.*, 39(2009), No. 6, p. 927.
[53] C. Nourry, L. Massot, P. Chamelot, and P. Taxil, Neodymium and gadolinium extraction from molten fluorides by reduction on a reactive electrode, *J. Appl. Electrochem.*, 39(2009), No. 12, p. 2359.
[54] A. Saïla, M. Gibilaro, L. Massot, P. Chamelot, P. Taxil, and A.M. Affoune, Electrochemical behaviour of dysprosium(III) in LiF–CaF_2 on Mo, Ni and Cu electrodes, *J. Electroanal. Chem.*, 642(2010), No. 2, p. 150.
[55] T. Nohira, S. Kobayashi, K. Kondo, K. Yasuda, R. Hagiwara, T. Oishi, and H. Konishi, Electrochemical formation of RE−Ni (RE = Pr, Nd, Dy) alloys in molten halides, *ECS Trans.*, 50(2013), No. 11, p. 473.
[56] Y.S. Yang, M.L. Zhang, W. Han, P.Y. Sun, B. Liu, H.L. Jiang, T. Jiang, S.M. Peng, M. Li, K. Ye, and Y.D. Yan, Selective electrodeposition of dysprosium in LiCl–KCl–$GdCl_3$–$DyCl_3$ melts at magnesium electrodes: Application to separation of nuclear wastes, *Electrochim. Acta*, 118(2014), p. 150.
[57] Y.C. Wang, M. Li, W. Han, M.L. Zhang, Y.S. Yang, Y. Sun, Y.C. Zhao, and Y.D. Yan, Electrochemical extraction and separation of praseodymium and erbium on reactive magnesium electrode in molten salts, *J. Solid State Electrochem.*, 19(2015), No. 12, p. 3629.
[58] D.B. Ji, T.Q. Yin, Y.D. Yan, M.L. Zhang, P. Wang, Y.H. Liu, J.N. Zheng, Y. Xue, X.Y. Jing, and W. Han, Electrochemical reduction La(III) on W and Mg electrodes: application to prepare Mg–La and Mg–Li–La alloys in LiCl–KCl melts, *RSC Adv.*, 6(2016), No. 35, p. 29353.
[59] X. Li, Y.D. Yan, M.L. Zhang, H. Tang, D.B. Ji, W. Han, Y. Xue, and Z.J. Zhang, Electrochemical reduction of Tm on Mg electrodes and co-reduction of Mg, Li and Tm on W electrodes, *Electrochim. Acta*, 135(2014), p. 327.
[60] Y. Chen, K. Ye, and M.L. Zhang, Preparation of Mg−Yb alloy film by electrolysis in the molten LiCl−KCl−$YbCl_3$ system at low temperature, *J. Rare Earths*, 28(2010), No. 1, p. 128.
[61] Z.S. Hua, J. Wang, L. Wang, Z. Zhao, X.L. Li, Y.P. Xiao, and Y.X. Yang, Selective extraction of rare earth elements from NdFeB scrap by molten chlorides, *ACS Sustain. Chem. Eng.*, 2(2014), No. 11, p. 2536.
[62] D.B. Ji, Y.D. Yan, M.L. Zhang, X. Li, X.Y. Jing, W. Han, Y. Xue, and Z.J. Zhang, Separation of lanthanum from samarium on solid aluminum electrode in LiCl–KCl eutectic melts, *J. Radioanal. Nucl. Chem.*, 304(2015), No. 3, p. 1123.
[63] K. Liu, Y.L. Liu, L.Y. Yuan, H. He, Z.Y. Yang, X.L. Zhao, Z.F. Chai, and W.Q. Shi, Electroextraction of samarium from Sm_2O_3 in chloride melts, *Electrochim. Acta*, 129(2014), p. 401.
[64] K. Liu, Y.L. Liu, L.Y. Yuan, X.L. Zhao, Z.F. Chai, and W.Q. Shi, Electroextraction of gadolinium from Gd_2O_3 in LiCl–KCl–$AlCl_3$ molten salts, *Electrochim. Acta*, 109(2013), p. 732.
[65] Y. Castrillejo, A. Vega, M. Vega, P. Hernández, J.A. Rodriguez, and E. Barrado, Electrochemical formation of Sc−Al in-

termetallic compounds in the eutectic LiCl–KCl. Determination of thermodynamic properties, *Electrochim. Acta*, 118(2014), p. 58.

[66] Y.L. Liu, L.Y. Yuan, G.A. Ye, L. Zhu, M.L. Zhang, Z.F. Chai, and W.Q. Shi, Co-reduction behaviors of lanthanum and aluminium ions in LiCl–KCl eutectic, *Electrochim. Acta*, 147(2014), p. 104.

[67] L. Wang, Y.L. Liu, K. Liu, S.L. Tang, L.Y. Yuan, L.L. Su, Z.F. Chai, and W.Q. Shi, Electrochemical extraction of cerium from CeO_2 assisted by $AlCl_3$ in molten LiCl–KCl, *Electrochim. Acta*, 147(2014), p. 385.

[68] M. Zhang, H.Y. Wang, W. Han, M.L. Zhang, Y.N. Li, Y.L. Wang, Y. Xue, F.Q. Ma, and X.M. Zhang, Electrochemical extraction of cerium and formation of Al–Ce alloy from CeO_2 assisted by $AlCl_3$ in LiCl–KCl melts, *Sci. China Chem.*, 57(2014), No. 11, p. 1477.

[69] H. Tang, H. Deng, Q.B. Ren, D.Z. Cai, Y.M. Ren, L. Shao, Y.D. Yan, and M.L. Zhang, Electrochemical behavior of praseodymium and Pr−Al intermetallics in LiCl−KCl−$AlCl_3$−$PrCl_3$ melts, *J. Rare Earths*, 34(2016), No. 4, p. 428.

[70] Y. Castrillejo, M. Bermejo, P.D. Arocas, A. Martínez, and E. Barrado, Electrochemical behaviour of praseodymium(III) in molten chlorides, *J. Electroanal. Chem.*, 575(2005), No. 1, p. 61.

[71] Y. Castrillejo, P. Fernández, J. Medina, P. Hernández, and E. Barrado, Electrochemical extraction of samarium from molten chlorides in pyrochemical processes, *Electrochim. Acta*, 56(2011), No. 24, p. 8638.

[72] D.B. Ji, Y.D. Yan, M.L. Zhang, X. Li, X.Y. Jing, W. Han, Y. Xue, Z.J. Zhang, and T. Hartmann, Electrochemical preparation of Al–Sm intermetallic compound whisker in LiCl–KCl Eutectic Melts, *Electrochim. Acta*, 165(2015), p. 211.

[73] M.R. Bermejo, F. De la Rosa, E. Barrado, and Y. Castrillejo, Cathodic behaviour of europium(III) on glassy carbon, electrochemical formation of Al_4Eu, and oxoacidity reactions in the eutectic LiCl–KCl, *J. Electroanal. Chem.*, 603(2007), No. 1, p. 81.

[74] M.R. Bermejo, J. Gómez, J. Medina, A.M. Martínez, and Y. Castrillejo, The electrochemistry of gadolinium in the eutectic LiCl–KCl on W and Al electrodes, *J. Electroanal. Chem.*, 588(2006), No. 2, p. 253.

[75] M. Li, Q.Q. Gu, W. Han, Y.D. Yan, M.L. Zhang, Y. Sun, and W.Q. Shi, Electrodeposition of Tb on Mo and Al electrodes: Thermodynamic properties of $TbCl_3$ and $TbAl_2$ in the LiCl−KCl eutectic melts, *Electrochim. Acta*, 167(2015), p. 139.

[76] Y. Castrillejo, M.R. Bermejo, A.I. Barrado, R. Pardo, E. Barrado, and A.M. Martinez, Electrochemical behaviour of dysprosium in the eutectic LiCl–KCl at W and Al electrodes, *Electrochim. Acta*, 50(2005), No. 10, p. 2047.

[77] L.L. Su, K. Liu, Y.L. Liu, L. Wang, L.Y. Yuan, L. Wang, Z.J. Li, X.L. Zhao, Z.F. Chai, and W.Q. Shi, Electrochemical behaviors of Dy(III) and its co-reduction with Al(III) in molten LiCl−KCl salts, *Electrochim. Acta*, 147(2014), p. 87.

[78] Y. Castrillejo, M.R. Bermejo, E. Barrado, J. Medina, and A.M. Martínez, Electrodeposition of Ho and electrochemical formation of Ho–Al alloys from the eutectic LiCl–KCl, *J. Electrochem. Soc.*, 153(2006), No. 10, p. C713.

[79] K. Liu, Y.L. Liu, L.Y. Yuan, L. Wang, L. Wang, Z.J. Li, Z.F. Chai, and W.Q. Shi, Thermodynamic and electrochemical properties of holmium and HoxAly intermetallic compounds in the LiCl−KCl eutectic, *Electrochim. Acta*, 174(2015), p. 15.

[80] Y. Castrillejo, M.R. Bermejo, E. Barrado, and A.M. Martínez, Electrochemical behaviour of erbium in the eutectic LiCl–KCl at W and Al electrodes, *Electrochim. Acta*, 51(2006), No. 10, p. 1941.

[81] K. Liu, Y.L. Liu, L.Y. Yuan, X.L. Zhao, H. He, G.A. Ye, Z.F. Chai, and W.Q. Shi, Electrochemical formation of erbium-aluminum alloys from erbia in the chloride melts, *Electrochim. Acta*, 116(2014), p. 434.

[82] Y. Castrillejo, P. Fernández, M.R. Bermejo, E. Barrado, and A.M. Martínez, Electrochemistry of thulium on inert electrodes and electrochemical formation of a Tm–Al alloy from molten chlorides, *Electrochim. Acta*, 54(2009), No. 26, p. 6212.

[83] X. Li, Y.D. Yan, M.L. Zhang, H. Tang, D.B. Ji, W. Han, Y. Xue, and Z.J. Zhang, Electrochemical formation of Al–Tm intermetallics in eutectic LiCl–KCl melt containing Tm and Al ions, *J. Nucl. Mater.*, 452(2014), No. 1-3, p. 197.

[84] Y. Castrillejo, P. Fernández, J. Medina, M. Vega, and E. Barrado, Chemical and electrochemical extraction of ytterbium from molten chlorides in pyrochemical processes, *Electroanalysis*, 23(2011), No. 1, p. 222.

[85] Y.D. Yan, X. Li, M.L. Zhang, Y. Xue, H. Tang, W. Han, and Z.J. Zhang, Electrochemical extraction of ytterbium and formation of Al–Yb alloy from Yb_2O_3 assisted by $AlCl_3$ in LiCl–KCl melt, *J. Electrochem. Soc.*, 159(2012), No. 11, p. 649.

[86] M.R. Bermejo, E. Barrado, A.M. Martínez, and Y. Castrillejo, Electrodeposition of Lu on W and Al electrodes: electrochemical formation of Lu–Al alloys and oxoacidity reactions of Lu(III) in the eutectic LiCl–KCl, *J. Electroanal. Chem.*, 617(2008), No. 1, p. 85.

[87] X. Li, Y.D. Yan, M.L. Zhang, Y. Xue, H. Tang, D.B. Ji, and Z.J. Zhang, $AlCl_3$ and liquid Al assisted extraction of Nd from NaCl–KCl melts via intermittent galvanostatic electrolysis, *RSC Adv.*, 4(2014), No. 76, p. 40352.

[88] Y. Ito and T. Nohira, Non-conventional electrolytes for electrochemical applications, *Electrochim. Acta*, 45(2000), No. 15, p. 2611.

[89] D.C. Jiles, The development of highly magnetostrictive rare earth-iron alloys, *J. Phys. D: Appl. Phys.*, 27(1994), No. 1, p. 1.

[90] H. Konishi, T. Nohira, and Y. Ito, Formation of Dy–Fe alloy films by molten salt electrochemical process, *Electrochim. Acta*, 47(2002), No. 21, p. 3533.

[91] H. Konishi, H. Hua, H. Ono, Y. Koizumi, T. Oishi, and T. Nohira, Electrochemical formation of Dy−Fe and Nd−Fe alloys in molten $CaCl_2$−LiCl systems, *ECS Trans.*, 86(2018), No. 14, p. 321.

[92] T. Iida, T. Nohira, and Y. Ito, Electrochemical formation of Sm–Co alloy films by Li codeposition method in a molten LiCl–KCl–$SmCl_3$ system, *Electrochim. Acta*, 48(2003), No. 7, p. 901.

[93] T. Kubota, T. Iida, T. Nohira, and Y. Ito, Formation and phase control of Co–Gd alloy films by molten salt electrochemical process, *J. Alloys Compd.*, 379(2004), No. 1-2, p. 256.

[94] H. Konishi, H. Ono, E. Takeuchi, T. Nohira, and T. Oishi, Electrochemical formation of RE−Cu (RE = Dy, Nd) alloys in a molten LiCl-KCl system, *ECS Trans.*, 53(2013), No. 11, p. 37.

[95] M. Li, B. Liu, N. Ji, Y. Sun, W. Han, T. Jiang, S.M. Peng, Y.D. Yan, and M.L. Zhang, Electrochemical extracting variable valence ytterbium from LiCl–KCl–$YbCl_3$ melt on Cu electrode, *Electrochim. Acta*, 193(2016), p. 54.

[96] W. Han, Z.Y. Li, M. Li, X. Hu, X.G. Yang, M.L. Zhang, and Y. Sun, Electrochemical behavior and extraction of holmium on Cu electrode in LiCl−KCl molten salt, *J. Electrochem. Soc.*, 164(2017), No. 13, p. D934.

[97] Y.C. Wang, M. Li, W. Han, M.L. Zhang, T. Jiang, S.M. Peng, and Y.D. Yan, Electrochemical behaviour of erbium(III) and its extraction on Cu electrode in LiCl−KCl melts, *J. Alloys Compd.*, 695(2017), p. 3484.

[98] W. Han, Z.Y. Li, M. Li, Y.Y. Gao, X.G. Yang, M.L. Zhang, and Y. Sun, Electrolytic extraction of dysprosium and thermodynamic evaluation of Cu–Dy intermetallic compound in eutectic LiCl–KCl, *RSC adv.*, 8(2018), No. 15, p. 8118.

[99] M. Li, J. Wang, W. Han, Y.C. Dong, W. Wang, M.L. Zhang, X.G. Yang, and Y. Sun, Recovery of terbium from LiCl−KCl−$TbCl_3$ system by electrodeposition using different electrodes, *J. Electrochem. Soc.*, 165(2018), No. 14, p. D704.

[100] Y.C. Wang, M. Li, M.L. Zhang, W. Han, T. Jiang, and Y.D. Yan, Electrochemical deposition of praseodymium(III) and copper(II) and extraction of praseodymium on copper electrode in LiCl−KCl melts, *J. Solid State Electrochem.*, 22(2018), No. 12, p. 3689.

[101] Y.C. Wang, Y.H. Liu, M. Li, W. Han, Y.B. Liu, and Y.H. Liu, Extraction of gadolinium on Cu electrode from LiCl−KCl melts by formation of Cu−Gd alloys, *Ionics*, 25(2019), No. 4, p. 1897.

[102] Y. Kamimoto, T. Itoh, K. Kuroda, and R. Ichino, Recovery of rare-earth elements from neodymium magnets using molten salt electrolysis, *J. Mater. Cycles Waste Manage.*, 19(2017), No. 3, p. 1017.

[103] Y. Kamimoto, T. Itoh, G. Yoshimura, K. Kuroda, T. Hagio, and R. Ichino, Electrodeposition of rare-earth elements from neodymium magnets using molten salt electrolysis, *J. Mater. Cycles Waste Manage.*, 20(2018), No. 4, p. 1918.

[104] Y. Kamimoto, G. Yoshimura, T. Itoh, K. Kuroda, and R. Ichino, Leaching of rare earth elements from neodymium magnet using electrochemical method, *Trans. Mater. Res. Soc. Jpn.*, 40(2015), No. 4, p. 343.

[105] W. Han, W.L. Li, M. Li, Z.Y. Li, Y. Sun, X.G. Yang, and M.L. Zhang, Electrochemical co-reduction of Y(III) and Zn(II) and extraction of yttrium on Zn electrode in LiCl−KCl eutectic melts, *J. Solid State Electrochem.*, 22(2018), No. 8, p. 2435.

[106] Y.L. Liu, L.Y. Yuan, K. Liu, G.A. Ye, M.L. Zhang, H. He, H.B. Tang, R.S. Lin, Z.F. Chai, and W.Q. Shi, Electrochemical extraction of samarium from LiCl−KCl melt by forming Sm-Zn alloys, *Electrochim. Acta*, 120(2014), p. 369.

[107] L. Wang, Y.L. Liu, K. Liu, S.L. Tang, L.Y. Yuan, T. Lu, Z.F. Chai, and W.Q. Shi, Electrochemical extraction of cerium by forming Ce−Zn alloys in LiCl−KCl eutectic on W and liquid Zn electrodes, *J. Electrochem. Soc.*, 162(2015), No. 9, p. E179.

[108] M. Li, J. Wang, W. Han, X.G. Yang, M. Zhang, Y. Sun, M.L. Zhang, and Y.D. Yan, Electrochemical formation and thermodynamic evaluation of Pr−Zn intermetallic compounds in LiCl−KCl eutectic melts, *Electrochim. Acta*, 228(2017), p. 299.

[109] L.X. Luo, Y.L. Liu, N. Liu, L. Wang, L.Y. Yuan, Z.F. Chai, and W.Q. Shi, Electrochemical and thermodynamic properties of Nd(III)/Nd(0) couple at liquid Zn electrode in LiCl−KCl melt, *Electrochim. Acta*, 191(2016), p. 1026.

[110] W. Zhou, Y.L. Liu, K. Liu, Z.R. Liu, L.Y. Yuan, L. Wang, Y.X. Feng, Z.F. Chai, and W.Q. Shi, Electroreduction of Gd^{3+} on W and Zn electrodes in LiCl–KCl eutectic: A comparison study, *J. Electrochem. Soc.*, 162(2015), No. 10, p. D531.

[111] Y.L. Liu, W. Zhou, H.B. Tang, Z.R. Liu, K. Liu, L.Y. Yuan, Y.X. Feng, Z.F. Chai, and W.Q. Shi, Diffusion coefficient of Ho^{3+} at liquid zinc electrode and co-reduction behaviors of Ho^{3+} and Zn^{2+} on W electrode in the LiCl−KCl eutectic, *Electrochim. Acta*, 211(2016), p. 313.

[112] X. Li, Y.D. Yan, M.L. Zhang, Y. Xue, H. Tang, Z.P. Zhou, X.N. Yang, and Z.J. Zhang, $ZnCl_2$ and liquid zinc assisted electrochemical extraction of thulium from LiCl−KCl melt, *J. Electrochem. Soc.*, 161(2014), No. 5, p. D248.

[113] P. Wang, D.B. Ji, D.Q. Ji, J.N. Zheng, Y.D. Yan, M.L. Zhang, W. Han, and H.J. Wu, Electrochemical and thermodynamic properties of ytterbium and formation of Zn−Yb alloy on liquid Zn electrode, *J. Nucl. Mater.*, 517(2019), p. 157.

[114] J.W. Pang, K. Liu, Y.L. Liu, C.M. Nie, L.X. Luo, L.Y. Yuan, Z.F. Chai, and W.Q. Shi, Electrochemical properties of lanthanum on the liquid gallium electrode in LiCl−KCl eutectic, *J. Electrochem. Soc.*, 163(2016), No. 14, p. D750.

[115] K. Liu, Y.L. Liu, Z.F. Chai, and W.Q. Shi, Evaluation of the electroextractions of Ce and Nd from LiCl−KCl molten salt using liquid Ga electrode, *J. Electrochem. Soc.*, 164(2017), No. 4, p. D169.

[116] B. Li, K. Liu, J.W. Pang, L.Y. Yuan, Y.L. Liu, and M.Z. Lin, Electrochemical properties of gadolinium on liquid gallium electrode in LiCl−KCl eutectic, *J. Rare Earths*, 36(2018), No. 6, p. 656.

[117] M. Li, Y.C. Liu, Z.X. Sun, W. Han, M.L. Zhang, X.G. Yang, and Y. Sun, Electrochemical co-reduction of Bi(III) and Y(III) and extracting yttrium from molten LiCl−KCl using liquid Bi as cathode, *Chem. Res. Chin. Univ.*, 35(2019), No. 1, p. 60.

[118] M. Li, Q.Q. Gu, W. Han, X.M. Zhang, Y. Sun, M.L. Zhang, and Y.D. Yan, Electrochemical behavior of La(III) on liquid Bi electrode in LiCl–KCl melts. Determination of thermodynamic properties of La–Bi and Li–Bi intermetallic compounds, *RSC Adv.*, 5(2015), No. 100, p. 82471.

[119] W. Han, Z.Y. Li, M. Li, W.L. Li, X.M. Zhang, X.G. Yang, M.L. Zhang, and Y. Sun, Electrochemical extraction of holmium and thermodynamic properties of Ho-Bi alloys in LiCl−KCl eutectic, *J. Electrochem. Soc.*, 164(2017), No. 4, p. E62.

[120] W. Han, N. Ji, J. Wang, M. Li, X.G. Yang, Y. Sun, and M.L. Zhang, Electrochemical formation and thermodynamic properties of Tb–Bi intermetallic compounds in eutectic LiCl–KCl, *RSC Adv.*, 7(2017), No. 50, p. 31682.

[121] S.S. Wang, B.C. Wei, M. Li, W. Han, M.L. Zhang, X.G. Yang, and Y. Sun, Electrochemical behavior of Dy(III) on bismuth film electrode in eutectic LiCl-KCl melts, *J. Rare Earths*, 36(2018), No. 9, p. 1007.

[122] Y. Ito, T. Nishikiori, and H. Tsujimura, Novel molten salt electrochemical processes for industrial applications, *Electrochemistry*, 86(2018), No. 2, p. 21.

[123] T. Oishi, M. Yaguchi, Y. Katasho, and T. Nohira, Separation of neodymium and dysprosium by molten salt electrolysis using an alloy diaphragm, [in] Azimi, K. Forsberg, T. ouchi, H. Kim, S. Alam, and A. Baba, eds., *Rare Metal Technology 2020*, Springer, Cham, 2020, p. 151.

[124] M. Itoh, K. Miura, and K. Machida, Novel rare earth recovery process on Nd–Fe–B magnet scrap by selective chlorination using NH_4Cl, *J. Alloys Compd.*, 477(2009), No. 1-2, p. 484.

[125] S. Shirayama and T.H. Okabe, Selective extraction and recovery of Nd and Dy from Nd–Fe–B magnet scrap by utilizing molten $MgCl_2$, *Metall. Mater. Trans. B*, 49(2018), p. 1067.

[126] Y.X. Chen, Research progress of preparation of rare earth metals by electrolysis in fluoride salt system, *Chin. Rare*

Earths, 35(2014), No. 2, p. 99.
[127] A. Abbasalizadeh, A. Malfliet, S. Seetharaman, J. Sietsma, and Y. Yang, Electrochemical recovery of rare earth elements from magnets: conversion of rare earth based metals into rare earth fluorides in molten salts, *Mater. Trans.*, 58(2017), No. 3, p. 400.
[128] Y.S. Yang, C.Q. Lan, L.Y. Guo, Z.Q. An, Z.W. Zhao, and B.W. Li, Recovery of rare-earth element from rare-earth permanent magnet waste by electro-refining in molten fluorides, *Sep. Purif. Technol.*, 233(2020), p. 116030.
[129] L. Massot, P. Chamelot, and P. Taxil, Cathodic behaviour of samarium(III) in LiF–CaF_2 media on molybdenum and nickel electrodes, *Electrochim. Acta*, 50(2005), No. 28, p. 5510.
[130] M. Gibilaro, L. Massot, P. Chamelot, L. Cassayre, and P. Taxil, Electrochemical extraction of europium from molten fluoride media, *Electrochim. Acta*, 55(2009), No. 1, p. 281.
[131] B.A. Frandsen, S.D. Nickerson, A.D. Clark, A. Solano, R. Baral, J. Williams, J. Neuefeind, and M. Memmott, The structure of molten FLiNaK, *J. Nucl. Mater.*, 537(2020), p. 152219.
[132] J.S. Zhang, Impurities in primary coolant salt of FHRs: Chemistry, impact, and removal methods, *Energy Technol.*, 7(2019), No. 10, p. 1900016.
[133] C. Hamel, P. Chamelot, and P. Taxil, Neodymium(III) cathodic processes in molten fluorides, *Electrochim. Acta*, 49(2004), No. 25, p. 4467.
[134] H.M. Zhu, Rare earth metal production by molten salt electrolysis, [in] G. Kreysa, K. Ota, and R.F. Savinell, eds., *Encyclopedia of Applied Electrochemistry*, Springer, New York, 2014, p. 1765.
[135] Y.F. Wang, J.B. Ge, W.Q. Zhuo, S.Q. Guo, and J.S. Zhang, Electrochemical separation study of LaF_3 in molten FLiNaK salt, *J. Nucl. Mater.*, 518(2019), p. 162.
[136] H. Qiao, T. Nohira, and Y. Ito, Electrochemical formation of Pd–La alloy films in a LiF–NaF–KF–LaF_3 melt, *J. Alloys Compd.*, 359(2003), No. 1-2, p. 230.
[137] M.H. Brooker, R.W. Berg, J.H. Von Barner, and N.J. Bjerrum, Raman Study of the hexafluoroaluminate ion in solid and molten FLINAK, *Inorg. Chem.*, 39(2000), No. 16, p. 3682.
[138] M.Y. Zhang, J.B. Ge, J.S. Zhang, and L.E. Liu, Redox potential measurement of AgCl in molten LiCl−KCl salt using chronopotentiometry and potentiodynamic scan techniques, *Electrochem. Commun.*, 105(2019), p. 106498.
[139] A. Roine, Chemical reaction and equilibrium software with extensive thermo-chemical database, *Outokumpu HSC 6.0*, 2010. https://www.hsc-chemistry.com/.
[140] Y.F. Wang, J.B. Ge, W.Q. Zhuo, S.Q. Guo, and J.S. Zhang, Electrochemical extraction of lanthanum in molten fluoride salts assisted by KF or NaF, *Electrochem. Commun.*, 104(2019), p. 106468.
[141] V. Constantin, A.M. Popescu, and S. Zuca, Preliminary studies of the obtaining of solid metallic cerium from fluoride melts, *J. Nat. Res. A*, 58(2003), No. 1, p. 57.
[142] V. Constantin, A.M. Popescu, and M. Olteanu, Electrochemical studies on cerium(III) in molten fluoride mixtures, *J. Rare Earths*, 28(2010), No. 3, p. 428.
[143] P. Fedorov, Systems of alkali and rare-earth metal fluorides, *Russ. J. Inorg. Chem*, 44(1999), No. 11, p. 1703.
[144] A. Grzechnik, N. Khaidukov, and K. Friese, Crystal structures and stability of trigonal $KLnF_4$ fluorides (Ln= Y, Ho, Er, Tm, Yb), *Dalton Trans.*, 42(2013), No. 2, p. 441.
[145] V. Dracopoulos, B. Gilbert, and G.N. Papatheodorou, Vibrational modes and structure of lanthanide fluoride–potassium fluoride binary melts LnF_3–KF (Ln=La, Ce, Nd, Sm, Dy, Yb), *J. Chem. Soc., Faraday Trans.*, 94(1998), No. 17, p. 2601.